catalysts

MDPI

Article

Design and Development of a Catalytic Fixed-Bed Reactor for Gasification of Banana Biomass in Hydrogen Production

Diego Tacuri, Christian Andrade, Paúl Álvarez, Mónica Abril-González, Silvana Zalamea, Verónica Pinos-Vélez, Lourdes Jara * and Andres Montero-Izquierdo *

Grupo de Ingeniería de Reactores, Catálisis y Tecnologías del Medio Ambiente, Departamento de Biociencias, Universidad de Cuenca, Cuenca 010202, Ecuador; diego.tacuri@ucuenca.edu.ec (D.T.); christian.andrade@ucuenca.edu.ec (C.A.); paul.alvarez@ucuenca.edu.ec (P.Á.); monica.abrilg@ucuenca.edu.ec (M.A.-G.); silvana.zalamea@ucuenca.edu.ec (S.Z.); veronica.pinos@ucuenca.edu.ec (V.P.-V.)
* Correspondence: lourdes.jara@ucuenca.edu.ec (L.J.); andres.montero@ucuenca.edu.ec (A.M.-I.)

Abstract: Hydrogen produced from biomass is an alternative energy source to fossil fuels. In this study, hydrogen production by gasification of the banana plant is proposed. A fixed-bed catalytic reactor was designed considering fluidization conditions and a height/diameter ratio of 3/1. Experimentation was carried out under the following conditions: 368 °C, atmospheric pressure, 11.75 g of residual mass of the banana (pseudo-stem), an average particle diameter of 1.84 mm, and superheated water vapor as a gasifying agent. Gasification reactions were performed using a catalyzed and uncatalyzed medium to compare the effectiveness of each case. The catalyst was Ni/Al_2O_3, synthesized by coprecipitation. The gas mixture produced from the reaction was continuously condensed to form a two-phase liquid–gas system. The synthesis gas was passed through a silica gel filter and analyzed online by gas chromatography. To conclude, the results of this study show production of 178 mg of synthesis gas for every 1 g of biomass and the selectivity of hydrogen to be 51.8 mol% when a Ni 2.5% *w*/*w* catalyst was used. The amount of CO_2 was halved, and CO was reduced from 3.87% to 0% in molar percentage. Lastly, a simulation of the distribution of temperatures inside the furnace was developed; the modeled behavior is in agreement with experimental observations.

Keywords: hydrogen; gasification; banana plant

Citation: Tacuri, D.; Andrade, C.; Álvarez, P.; Abril-González, M.; Zalamea, S.; Pinos-Vélez, V.; Jara, L.; Montero-Izquierdo, A. Design and Development of a Catalytic Fixed-Bed Reactor for Gasification of Banana Biomass in Hydrogen Production. *Catalysts* **2022**, *12*, 395. https://doi.org/10.3390/catal12040395

Academic Editors: Qinghua Lai, Qingfeng Zhang and Run-Ping Ye

Received: 26 February 2022
Accepted: 28 March 2022
Published: 1 April 2022

1. Introduction

The constant population growth of the last few decades has created an economic, demographic, and energy-demand paradigm of global proportions [1] This growth has triggered serious environmental problems due to the increased consumption of fossil fuels, which increases greenhouse gas emissions and aggravates climate change. This situation has led researchers to seek clean energy alternatives to fossil fuels such as hydrogen production from renewable resources [2]. Consumption of renewable energy will double, and the share of renewables in the world's energy consumption is expected to increase from 11% in 2010 to 15% in 2040 [3].

Renewable hydrogen is a promising energy carrier for the future energy supply. According to the International Energy Agency, renewable hydrogen can become competitive by 2030 with a reduction in the production cost of around three times of actual cost [4]. Its benefits as an ecological, versatile, and efficient fuel, reflect the great potential to achieve a green and sustainable future, which is why its production has increased in recent years [5]. Hydrogen is considered a fuel that produces water as a by-product and is also versatile and carbon-free. One of the most important properties is its high energy density (122 MJ/kg), which gives it the ability to meet the energy demands set by the consumption of fossil fuels; in addition, it can be used as an energy carrier, a storage medium, and in fuel cells.

Generally, when electricity is compared with hydrogen, electricity has disadvantages of transmission and heat loss caused by high voltages and electrical resistance while hydrogen offers some advantages, such as high energy conversion effectiveness, ability to be created with zero emissions from water, long-distance transport, availability of storage options, and conversion to fuels [6,7].

Approximately 96% of the hydrogen produced today is generated from fossil fuels (natural gas, coal, and oil), in particular, through processes such as steam methane reforming (SMR) of natural gas, autothermal reforming, partial oxidation, and coal gasification; these processes are generally called gray hydrogen pathways [8,9]. This production is responsible for 6% of all natural gas consumption worldwide; however, greenhouse gas emissions are high; for this reason, the natural gas industry is promoting "blue hydrogen", which is a relatively new concept and can burn to hydrogen produced through SMR from natural gas or coal gasification but with carbon dioxide capture and storage. To date, there are no studies that analyze the methane emissions associated with the production of the natural gas necessary to generate blue hydrogen, considering that methane is a powerful greenhouse gas that could be counterproductive to this process [10]. In addition, hydrogen can also be generated by the electrolysis of water; when said electricity is produced by a clean and renewable source, such as hydroelectric, wind, or solar, it is called "green hydrogen". While current costs remain higher than fossil fuel-based solutions, it is expected that as the cost of renewables declines and electrolyzers become more efficient, this will be a viable solution to meet energy demands in future decades [8–10].

Hydrogen can be produced from renewable energy sources through various routes and methods [11]. Biomass is a sustainable resource that can be used to produce hydrogen through biomass gasification processes, steam, thermochemical conversion, etc. The former is the most promising to produce synthesis gas with high amounts of hydrogen. There is a wide variety of biomass resources, with different physical and chemical characteristics, resulting in unique and different steam gasification efficiencies. Water vapor is a gasifying agent that, in addition to producing synthesis gas with high percentages of H_2, it can reduce environmental impacts, generating low amounts of CO_2 and preventing the formation of NOx compounds. Biomass is characterized by (1) chemical composition (lignin, cellulose, and hemicellulose), (2) inherent mineral content, (3) elemental composition, and (4) physical properties (size, shape, density of particles) [12]. There are various applications of hydrogen, among the most important of which are fuels in internal combustion engines, fuel cells, maritime transport vehicles, chemical industries, etc. [13]. Currently, countries such as Japan, the United States, and China are implementing hydrogen as a source of energy in fuel cell buses [14]. Companies such as Hyundai and Toyota have unveiled their hydrogen-powered sports cars [15]. Hydrogen technology is making great strides, ushering in the hydrogen era. Biomass is considered the main source of renewable energy generation, since it acts as a natural battery, storing the sun's energy in the form of chemical bonds [13].

The net decrease in greenhouse gas emissions by replacing fossil fuels with biomass conversion technologies such as pyrolysis and gasification has been deeply studied to promote the use of renewable energies that partially solve environmental problems. Fixed-bed reactor gasification technologies are the most widely used for the energy conversion of urban solid waste and different types of biomasses [2]. Table 1 shows some examples of various investigations that use fixed-bed reactors; in addition, the reaction conditions and the results obtained to produce hydrogen are specified.

Table 1. Description of fixed-bed reaction systems.

Reaction System	Biomass	Catalyst	Reaction Conditions	Hydrogen Production, mg H_2/g Biomass	Ref.
Two-stage fixed-bed reaction system for catalytic gasification. (Pyrolysis and gasification)	Wood sawdust	Ni/MCM-41 Catalyst: 0.25 g	Wood sawdust: 0.8 g Pyrolysis: 530 °C T: 800 °C	42.52	[16]
Laboratory-scale gasification equipment: fixed-bed downdraft gasifier system	Corn straw	Blast furnace gas ash (BFGA)	Water vapor flow rate: 0.55 kg/h Gasification T: 950 °C	92.08	[17]
Two-stage fixed-bed reaction system for catalytic gasification. (Pyrolysis and gasification)	Wheat straw	Biochar from cotton stalk (CC). Ni/CC	T: 800 °C S/B [1] = 4 Ni: 15 wt.%	27.61–42.48	[18]
Updraft gasifier with a continuous biomass feeder	Pine sawdust	-	T: 800 to 950 °C. S/B: 2.05	45.05–135.40	[19]
Combined fixed-bed reactor	Palm oil wastes	Supported nano-NiLaFe/ ɣ-Al_2O_3	T: 800 °C, S/B ratio = 1.33 Particle size: 0.15–2 mm gas yield: 1.21–2.11 m^3/kg feed rate:0.3 kg/h.	101.78 39.75 (no catalyst)	[20]
Updraft gasifier	Lignocellulose	-	T: 900 °C S/B: 0.08–0.16	37.5	[21]
Gasification reactor	Fir sawdust	Eutectic blend of lithium, sodium, and potassium carbonates	T: 750 °C S/B: 1	72.60	[22]

S/B [1]: steam/biomass ratio.

For the gasification process, the main reactors used are updraft gasifier, downdraft gasifier, bubbling fluidized bed, circulating fluidized bed, and entrained flow bed. The thermal conversion efficiency of the downdraft gasifier is high, but its CO and H_2 production capacity are comparatively low. As for the downdraft gasifier, the high carbon conversion efficiency is appreciable, and it is less sensitive to the carbon and tar content of the fuel; therefore, it accepts materials with different characteristics. The fluidized-bed reactor and the entrained flow reactor produce a gas mixture containing a small amount of charcoal, tar, and CO_2. The feed particle size plays an absolute partitioning role between various gasifiers. Entrained flow gasifier requires extremely small particle size, and it is also strictly necessary to maintain feedstock size in the case of other gasifiers, such as the circulating fluidized bed, which only accept attenuated solid feedstock within the 100 mm dimension range. Temperature also shows various impacts on different systems. The downdraft gasifier has high temperature-control efficiency. It is necessary to keep the process temperature relatively low in the bubbling bed gasifier to avoid the removal of fluids from the bed. On the other hand, in the entrained flow gasifier, the high temperature and pressure of the process enable high throughput and fast feed conversion. Carbon loss with ash and ash slag also affects entrained flow gasifier performance. The same trend has also been found in the case of the bubbling fluidized-bed gasifier. As for the investment cost of the updraft gasifier, it is low, while that of the fluidized gasifier and the entrained flow gasifier is very high [21,23–31].

In addition to the synthesis of gas, other compounds such as tars and char were also obtained in the gasification process. The amount depends on various factors such as operating conditions, fuel composition, and gasifier hydrodynamics. Tar can lead to serious operational problems in downstream equipment such as coolers, filters, and channels imposing much cost on the system. Thus, tar control and removal are vital issues for the development of biomass gasification on an industrial scale [32]. One of the most promising methods for tar removal is through the application of homogeneous and heterogeneous catalysts. This application also contributes to reducing the activation energy necessary for the production of hydrogen [33].

Heterogeneous catalysts (especially supported Ni-based catalysts) have become the focus of gasification in recent years, for their high activity and relatively low cost. In addition, the supports that have presented the best yields for the production of hydrogen are MgO, Al_2O_3, and carbon nanotubes (CNTs). The high activity of these catalysts is attributed to the large metal surface area and high thermal stability [33–35].

However, despite the important advances in research achieved to date, none has managed to achieve a process for the generation of biofuels that is economically profitable, so that it can be applied on a large scale [36]. All recent, industrially developed, gasification-based, biomass-to-liquid (BTL) concepts have used either entrained flow gasification of pretreated biomass or fluidized-bed gasification, followed by secondary treatment of tars and hydrocarbon gasses [36].

As a complement to reactor design, simulation programs are often used contributing significantly to the decrease in design, validation, improvement, and production times at an industrial level [37]. As an example of this complementation, the distribution of temperatures inside a furnace, containing a catalytic reactor, is a process that deserves to be studied and characterized by numerical techniques, given the difficulties that represent the measurement of these temperatures by physical elements such as thermocouples and others [38].

The objective of this study is to design and test a fixed-bed gasification system to produce hydrogen, using an updraft approach, where the biomass is banana pseudo-stem packed under the catalyst bed. The catalysts used were Ni supported on Al_2O_3, at different concentrations for their activity and stability for H_2 production from biomass via gasification. The results of the catalytic and non-catalytic reactions were compared. Stable and continuous operation of the gasifier was expected in the experiments to obtain a higher hydrogen production. These results will provide good points of reference for the design of a gasification system at scale. In addition, a simulation of the temperature distribution in the system is carried out, which will allow new information to be obtained without experimental processes.

2. Results and Discussion

2.1. Design of the Gasification Reactor

According to the design equations described in Table 1 for the biomass bed and the catalyst bed, the results obtained are shown in Table 2. It is observed that the amount of biomass used versus that of the catalyst has a ratio of 3:1. Steam was used as the gasifying agent in which density and dynamic viscosity were calculated at the mean reaction temperature of 368 °C and were 2.32 kg/m^3 and 3.52 × 10^{-5} Pa.s, respectively.

Table 2. Reactor design parameters.

Parameter	Biomass Bed	Catalytic Bed
Bed height (cm)	5.6	1.011
Amount (g)	11.75	3.92
Average diameter of particles (mm)	1.84	0.074
Porosity	0.4	0.196

Prior to the gasification reaction, the system was preheated for 30 min at a temperature of 300 °C. Subsequently, the steam stream was introduced until reaching thermal equilibrium. Currently, the temperature of the surface of the reactor was equal to the temperature inside the furnace. Through the measurements carried out, it was determined that the equilibrium temperature was 640 °C and the time in which it was reached was 90 min.

With the reactor design equations, it was found that the minimum fluidization speed for the biomass bed was much higher than that of the catalytic bed; 0.18 m/s and 1.94×10^{-4} m/s, respectively. This is because the ratio of the mass of banana residue to the amount of catalyst used was 3 to 1. With this consideration, it was determined that the porosity of the fluidized bed (equal to 0.63) and the catalyst particles when fluidizing reached a height of 2.2 cm. As a result of the calculations, the values of different parameters were found; for instance, the minimum height of the equipment (height of the biomass bed added to the height of the fluidized bed of the catalyst) was equal to 0.078 m, while the total height of the equipment with oversizing was considered equal to 0.09 m. A height/diameter ratio equal to 3 was determined, whereby the total diameter of the reactor was equal to 3 cm. The estimated dimensions complied with all those established for the design of equipment. This ensured the proper functioning of the gasifier, in addition to allowing the gasification reaction to occur selectively toward the formation of hydrogen. The scheme of the final reaction system is shown in Figure 1.

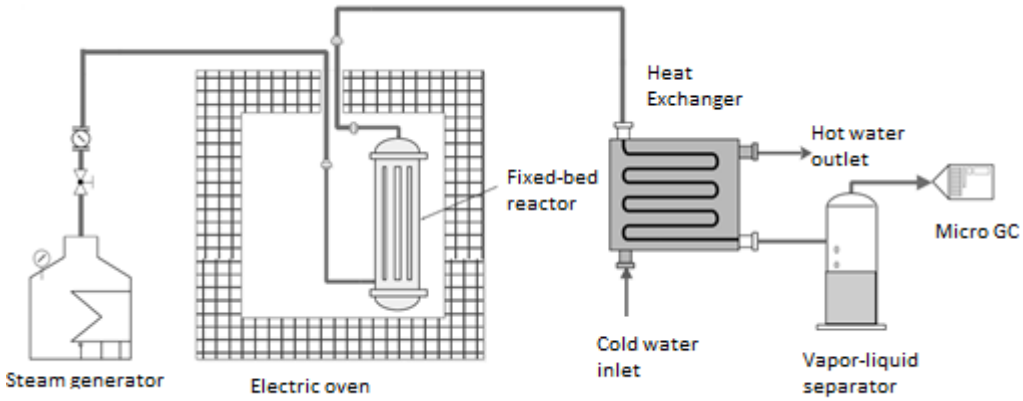

Figure 1. Reactor scheme.

2.2. Results of the Biomass Gasification Reaction

The gasification of the banana residues was carried out in a catalyzed and uncatalyzed reaction. Preliminary tests were carried out with the different catalyst compositions based on nickel (1.5, 2.5, and 5%). The result was 28.23, 51.78, and 25.50 in terms of hydrogen molar composition, respectively. It is shown that the best hydrogen production results were obtained with the catalyst synthesized with 2.5% nickel. These values are shown in Table 3.

Table 3. Molar composition of synthesis gas obtained with and without catalyst.

Component	**Ni/Al_2O_3%**			
% Molar	**0%**	**1.5%**	**2.5%**	**5%**
Hydrogen	25.79	28.23	51.78	25.50
Methene	2.21	1.01	0.44	2.28
Carbon monoxide	3.87	0.00	0.00	9.34
Carbon dioxide	47.15	45.38	22.54	39.40
Ethylene	20.32	24.64	25.01	22.42
Ethane	0.14	0.14	0.03	0.29
Acetylene	0.39	0.36	0.06	0.63
n-propane	0.14	0.15	0.06	0.15

The final gaseous product (syngas) was composed mainly of CO, CO_2, H_2, H_2O, CH_4, and N_2, with CO, CO_2, CH_4, and H_2 as the main groups of gasses due to their high performance, high calorific value, and their direct influence on the quality of the synthesis gas. A small number of C_2-C_4 components were classified as minor gasses. Nitrogen and oxygen did not participate in the gasification reaction. Therefore, they were excluded because they dilute the concentration of the other substances in the synthesis gas [39].

As seen in Table 3 and Figure 2, the composition of the synthesis gas changed significantly when the catalyst was used. Without a catalyst, the components that were found in the highest percentage were carbon dioxide > hydrogen > ethylene. In contrast, when the reaction was catalyzed with nickel, the gases with the highest content were hydrogen > ethylene > carbon dioxide.

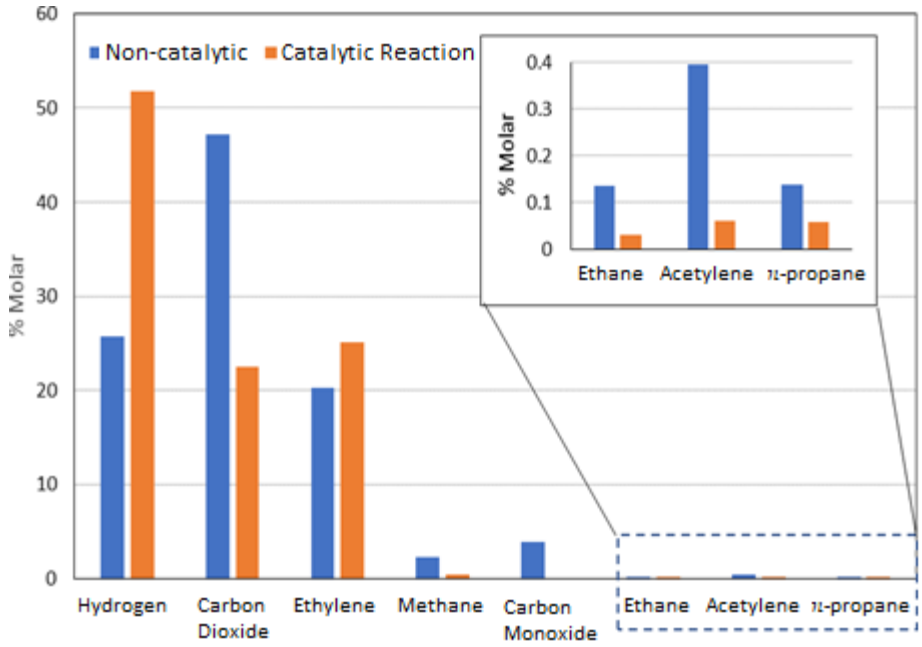

Figure 2. Molar percentage of synthesis gas obtained with and without catalyst.

This study confirms the good selectivity of the Ni catalyst toward H_2 formation. As the most relevant result of this study, it was demonstrated that the addition of the catalyst with a nickel content of 2.5% w/w caused hydrogen and ethylene to increase their molar content by 100% and 25%, respectively, while all the other elements decreased their mole percentage. One of the main reasons for the formation of ethylene is that the reaction temperature exceeded 600 °C [17,20]. The increase in the Ni load in the catalyst improves the conversion of carbon and the formation of H_2; however, an excessive increase also favors the formation of coke and with it the decrease in the yield of the reaction toward hydrogen [35]. In addition, the molar content of CO_2 was reduced by 50%. This can be justified by the dry-reforming reaction of methane, during which carbon dioxide (CO_2) reacts with the methane (CH_4) formed to generate carbon monoxide (CO) and hydrogen (H_2). This result showed that this reaction predominates when steam is used as a gasifying agent and Ni-based catalysts, which would explain the reduction in the amount of CO_2 [16].

It can also be seen that the carbon monoxide (CO) content was removed from the synthesis gas with the addition of the catalyst. The reduction was from 3.87% to 0% in mole percent. This behavior has been reported in other studies, which is because the Ni catalyst has a catalytic effect on the gas–water exchange reaction [20].

Comparing the results obtained in this study with different methods applied for the production of hydrogen, it is worth highlighting several findings: through plasma generation in banana waste using pure water, Putra et al. revealed that lignocellulose contents were decomposed into various gas products, and the highest hydrogen production

rate at 13.33 mg/g was found from banana pseudo-stem, at 3 wt% initial concentration [40]. On the other hand, Nathoa et al. applied a two-phase anaerobic digestion method for banana peel and found that hydrogen and methane yields reached values of 18.87 mg/g and 284.1 mL/g, respectively [41]. Through catalytic gasification, the results presented in Table 2 indicate that hydrogen production ranges from 27.61 to 101.78 mg/g, and the value obtained in this investigation is within this range. Although the result achieved is not optimal, this research is considered as a basis that, through subsequent studies, helps to improve the yield toward hydrogen production, as well as the profitability of the process, providing an alternative for the use of a biomass that is generated in large volumes.

In this study, the gas–water exchange reaction, the methane dry-reforming reaction, and the ethylene formation reaction may be predominant and explain the reduction in carbon dioxide and the increase in hydrogen and ethylene in the syngas [42]. In addition, the equipment and catalyst design improved the hydrogen/carbon monoxide ratio to a value of 6.67.

2.3. Analysis of the Calorific Value of Syngas

The upper and lower calorific value (PCS, PCI, respectively) of the synthesis gas obtained was estimated according to the equations described by [43], and the results are shown in Table 4. It is observed that both the PCS and the PCI of the synthesis gas obtained with the catalyst were 50% higher than that obtained without the catalyst; this is due to the increase in the H_2 content and the reduction in CO_2. The PCS and PCI results were also compared with commercial liquefied petroleum gas (LPG) in Ecuador, which has a calorific value 2.33 times higher than the synthesis gas obtained in this study. The low calorific value of the synthesis gas is due to the presence of non-oxidizing gasses, especially CO_2, which was approximately 25%.

Table 4. The upper and lower calorific values of the synthesis gas obtained in catalyzed and uncatalyzed reactions and the comparison of their LPG values.

Parameter	Catalyzed Reaction	Uncatalyzed Reaction	LPG	Ref.
PCS (kcal/kg)	5057.04	3342.5	11,800	[44]
PCI (kcal/kg)	4604	3077.43	10,830	[45]

The production of hydrogen is intensive in terms of energy consumption. To generate 1 kg of H_2, 60 kW of electrical energy is needed [46]. Currently, the hydrogen production costs from biomass are high, ranging from 1.21 to 2.42 USD/kg when using gasification, in contrast to 0.75 USD/kg with technologies such as steam methane reforming (SMR) based on natural gas to produce hydrogen [47]. In terms of CO_2 emissions, the use of biomass for hydrogen production represents a feasible path for energy transition according to IEA and its Net Zero Emissions for 2050 Scenario [48].

2.4. Temperature Distribution Simulation

Through the numerical simulation developed, the value reaching the surface of the reactor wall was 639.81 °C, while the data measured with the thermocouple gave a steady-state result of 639.41 °C. The calculated error was 0.06%. The air temperature inside the oven and the surface temperature of the reactor were measured using a pyrometer. The temperature of the air in the oven, the surface temperature of the reactor, and the tube were measured using a digital pyrometer, while a bimetallic thermometer was used for the temperature at the outlet of the reactor. These results are shown in Table 5.

Table 5. Experimental temperature data in °C.

Time (min)	Air Temp. Inside the Oven (T_A)	Reactor Surface Temp. (T_{RS})	Tube Surface Temp. (T_{TS})	Reactor Outlet Temp. (T_{OUT})
30	640	621.98	659.9	368.75
60	640	636.13	663.15	382.9
90	640	639.41	667.62	386.2

Figure 3 shows the temperature distribution in the furnace and the reactor body using the ANSYS Student version 2020R software.

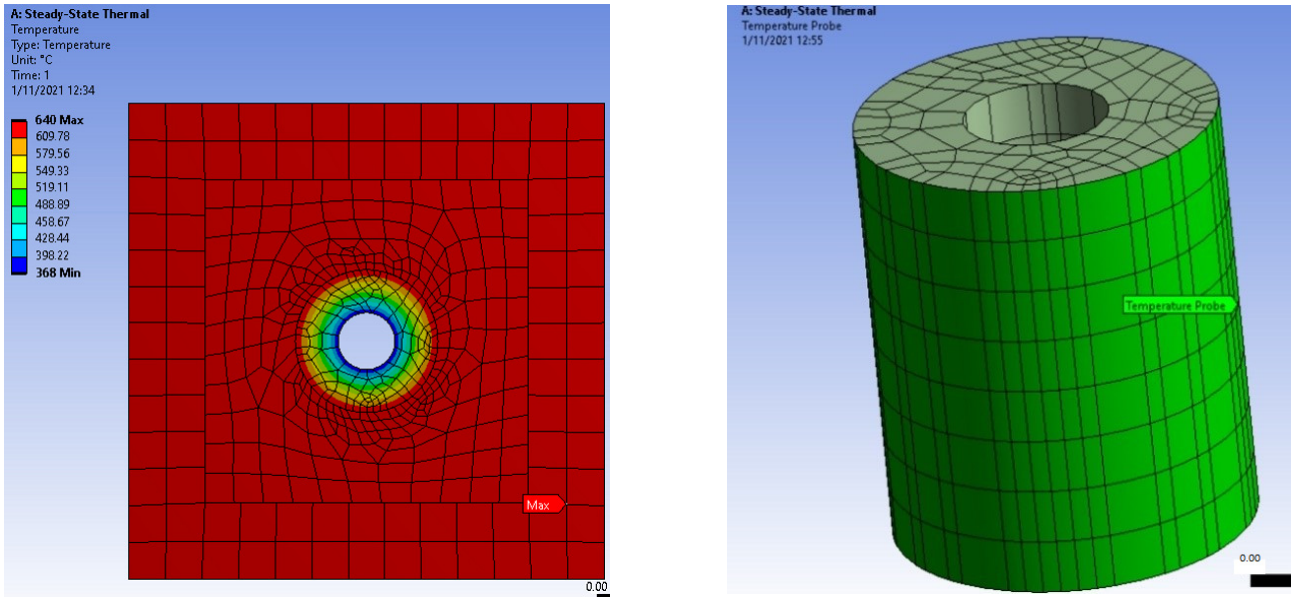

(**a**) (**b**)

Figure 3. Temperature distribution in the furnace and in the reactor body: (**a**) furnace distribution temperature; (**b**) reactor body temperature.

A second numerical simulation model in a transitory state was carried out to verify that the experimental data are correct in the experimentation over time. As a result of this simulation, it was found that, at time 0, the temperature inside the reactor was equal to that of the steam (95 °C). However, as time passed, it was found that the temperature of the internal surface of the reactor reached equilibrium at 509 °C, forming an asymptote at this value until completing the reaction time. Additionally, it was found that the steam temperature reached the value of 334.20 °C in a time of 360 s, as can be seen in Figure 4, and whose values reached equilibrium at 368 °C, as obtained experimentally. With these results, it was verified that the experimentally measured temperature values corresponded to the values obtained through the simulations carried out.

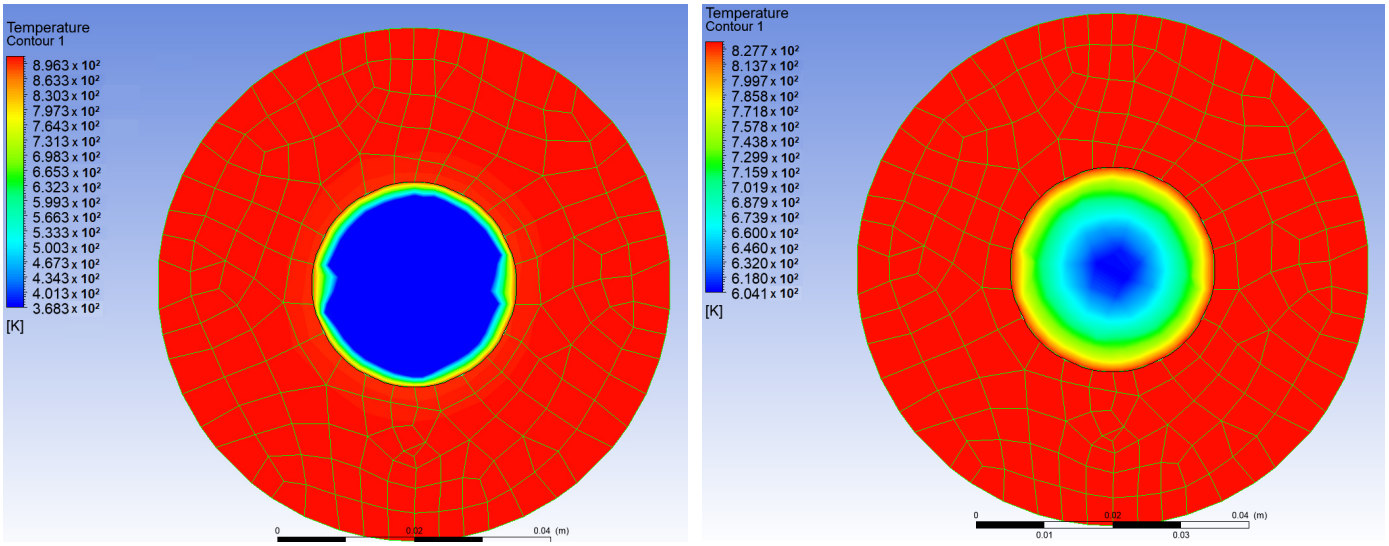

(**a**) (**b**)

Figure 4. Evolution of the temperature distribution in the center of the reactor from 0 to 360 s: (**a**) temperature distribution at 0 s; (**b**) temperature distribution at 360 s.

3. Materials and Methods

3.1. Sample Preparation

The biomass used was the pseudo-stem of the banana plant, reported as the one that is generated in the greatest quantity and from which the highest proportion of monosaccharides is obtained through hydrolysis processes [49]. It was obtained from the crops of "Hacienda La Clementina", which is one of the largest banana plantations in Ecuador. It is in the province of Los Ríos, whose latitude, and longitude are −1.710413008415544, −79.39049448451829, respectively. The banana variety used was Musa Acuminate, the Cavendish subgroup of the AAA Group, due to higher production in the country. This biomass was pretreated by a drying process at 105 °C for 24 h, until constant weight, its size was continuously decreased by grinding, and finally, it was sieved to reach a particle size between 1.69 to 2 mm. Equation (1) is used to calculate the mean diameter of the banana biomass particle. This equation has Xi represented as the fraction retained in the sieve and Di as the pore diameter of the sieve used [50].

$$D_p = \frac{1}{\sum \frac{x_i}{D_i}} \quad (1)$$

3.2. Reactor Design

A fixed-bed reactor with an upward flow was designed. It was initially proposed with two constraint variables: a bed height (hb) of 5.6 cm and a catalytic bed height (hc) of 10.11 mm. The length and diameter of the reactor were estimated considering a 3/1 ratio (length/diameter) as a design recommendation, resulting in a reactor 9 cm high and 3 cm in diameter.

To define the best construction and operating conditions for the reactor, individual analyses of a catalyzed and uncatalyzed gasification reaction were carried out. The equations are shown below. The material used for the construction of the reaction system was steel 340. In addition to the reactor, auxiliary equipment was used—namely, a boiler, an electric furnace, a heat exchanger, and a two-phase separator.

Description	Formula	Equation
Biomass amount	$m_b = h_0\ (1 - \varepsilon_O)\ \rho_P\ A$	(2)
Catalyst amount	$m_c = \frac{m_b}{3}$	(3)
Minimum fluidization speed	$v_{cr} = \frac{Re_{cr}\ \mu}{D_p\ \rho_m}$ $Re_{cr} = \frac{Ar}{\frac{150\ (1-\varepsilon_o)}{{\varepsilon_o}^3} + \sqrt{\frac{1.75}{{\varepsilon_o}^3}\sqrt{Ar}}}$ $Ar = \frac{{D_p}^3\ \rho_m\ g\ (\rho_p - \rho_m)}{\mu^2}$	(4)
Working speed ratio	$k_w = \frac{v_w}{v_{cr}}$	(5)
Fluidized-bed porosity	$Re_{LF} = k_w\ Re_{cr}$ $\varepsilon_{LF} = \left(\frac{18\ Re_{LF} + 0.36\ {Re_{LF}}^2}{Ar}\right)^{0.21}$	(6)
Fluidized-bed height	$h_{LF} = \frac{h_o\ (1-\varepsilon_o)}{(1-\varepsilon_{LF})}$	(7)
Total height of the gasification reactor	$H_{eq} = 3h_{LF}$	(8)
m_b = biomass amount (kg) m_c = catalyst amount (kg) ε_O = biomass bed porosity ρ_P = banana biomass particle density (kg/m^3) A = cross − sec tional area of the reactor (m^2) Ar = Archimedean dimensional number Re_{cr} = Critical Reynolds dimensional number D_p = mean biomass particle diameter (m) μ = dynamic viscosity of the gasifying agent (Pa s) H_{eq} = Total height of the gasification reactor (m)	ρ_m = gasifying agent density (kg/m^3) g = gravity acceleration (m/s^2) ρ_p = absolute density of a particle (kg/m^3) k_w = Working speed ratio v_w = initial fluid velocity (m/s) v_{cr} = critical velocity (m/s) Re_{LF} = Reynolds dimensional number in fluidization ε_{LF} = Fluidized-bed porosity h_o = Height bed particles in the fixed state (m)	

Information was taken from [51].

3.3. Catalyst Preparation

The catalysts were synthesized by coprecipitation following the method [52], by means of a continuous coprecipitation of $Ni(NO_3)_2.6H_2O$ and $Al(NO_3)_3.9H_2O$ in a 1M solution. Briefly, the reaction was carried out with constant stirring for 1 h, using an alkaline solution of Na_2CO_3 (2M) at constant temperature and pH: 50 °C and 8.01, respectively. The precipitated material was collected, filtered, and washed with deionized water (50 S conductivity). The resulting material was dried in an oven for 12 h at 80 °C and then calcined in a muffle at 600 °C for 6 h. All reagents used were purchased from Sigma Aldrich. Catalysts were prepared for three proportions of Ni, that is 1.5, 2.5, and 5% *w*/*w*.

3.4. Gasification Reaction

The gasification reaction was carried out at atmospheric pressure in the fixed-bed reactor designed for this investigation. The reaction system was heated with a resistive electric furnace. In addition, steam was used as a gasifying agent whose density and dynamic viscosity were calculated at the mean reaction temperature, which was measured over time at 4 specific points: inside the furnace (T_A), the surface of the pipe in the reheating zone (T_{TS}), the reactor surface (T_{RS}), and synthesis gasses at the outlet of the reactor (T_{OUT}).

The test started with a non-catalytic reaction. Briefly, 11.75 g of pretreated biomass was fed to the reactor. To avoid particle carryover and pack the biomass bed, 2 Tyler # 80 grids were used. Initially, the reaction system was preheated to a temperature of 300 °C. Consequently, a steam flow of 26 mL/min was continuously fed through a flow controller with a pressure of 7.5 PSI measured with a manometer, until reaching a reaction temperature of 368 °C. The established heating rate was 0.43 °C/s. The condensates were retained in a low-temperature heat exchanger located at the outlet of the reactor. The gaseous products were filtered and continuously analyzed on a Micro GC.

A set of catalytic reactions were carried out under the same conditions as the non-catalytic reaction. On the packed bed of biomass, 3.92 g of catalyst (ratio of biomass to catalyst; 3:1) was placed packed between two Tyler 200 grids to avoid carryover. Furthermore, the catalyst and biomass were placed in a fixed bed supported by quartz wool. The

resulting gasses were filtered and analyzed in the equipment. The selectivity for the formed products, and the hydrogen conversion, were calculated based on the following equations:

$$\%H_2\ selectivity = \frac{H_2\ moles\ produced}{\sum C_i\ moles} \cdot 100 \tag{9}$$

$$\%\ Selectivity\ of\ C_i = \frac{C_i\ moles\ produced}{\sum C_i\ moles} \cdot 100 \tag{10}$$

3.5. Synthesis Gas Analysis Method

The resulting gas was filtered with silica gel to remove possible moisture and then taken to the Micro GC equipment for dry analysis. Syngas analysis was performed online on an Agilent 490 Micro Gas Chromatograph. The software used for the compilation of results was Agilent 6890. The samples from the uncatalyzed and catalyzed reactions with the catalysts corresponding to 1.5%, 2.5%, and 5% by weight in Ni were analyzed.

3.6. Temperature Distribution Simulation

Heat conduction is the transfer of energy from the most energetic particles of a substance to the closest ones that have less energy; therefore, it can occur in solids, liquids, and gasses. It should also be noted that conduction of heat occurs in the direction of the highest temperature; its equation in the most general form using rectangular coordinates is

$$\frac{\partial^2 T}{\partial x^2} + \frac{\partial^2 T}{\partial y^2} + \frac{\partial^2 T}{\partial z^2} + \frac{g}{k} = \frac{1}{\alpha}\frac{\partial T}{\partial t} \tag{11}$$

where T is temperature, g is heat generation, k is the constant material thermal conductivity, and α is thermal diffusivity.

The case study corresponds to the furnace reactor and catalytic fixed bed where it is intended to study the heat transfer from the furnace air chamber to the walls of the reactor in steady state without heat generation for the two-dimensional case since, according to the geometry of the system, the hypotheses of symmetry can be used.

Considering the previous hypotheses, Equation (11) can be reduced to

$$\frac{\partial^2 T}{\partial x^2} + \frac{\partial^2 T}{\partial y^2} = 0 \tag{12}$$

The boundary conditions for the model under analysis are those that define the values of the temperature in the contour Γ (Dirichlet condition), as well as the condition of heat flow that exits in the direction normal to the contour Γq and that is prescribed (a condition from Neumann).

$$T - \underline{T} = 0\ en\ \ \Gamma\ T \tag{13}$$

$$q_n = \underline{q}_n \quad en\ \ \Gamma\ q \tag{14}$$

The numerical methodology used to solve this problem is applying the discretization of the domain by finite elements through the weak form obtained through the Galerkin weighted residuals method. For the analysis by means of finite elements, a three-dimensional model was used to carry out a thermal study of heat conduction for which boundary conditions were placed according to those that had been measured by thermocouples placed in the prototype. The materials used in the reactor simulation and their properties are shown in Table 6.

Table 6. Properties of the materials used in the reactor simulation.

Properties	Reactor (AISI 1020 A Steel)	Furnace Wall (Glass Wool Insulation)
Density (kg/m^3)	7870	20
Thermal conductivity (W/m·K)	51.9	0.03
Specific heat capacity (J/g·K)	0.486	840
Coefficient of thermal expansion (1E-6/K)	11.7	4.8

The equations used in these simulation models are mainly based on the steady-state and transient-state heat conduction equations, with constant thermal conductivity [53]. To complement the study, the reactor was modeled in a transient state with solid–liquid interface, using the ANSYS workbench interface and CFX solver. The model was composed of the body of the reactor (thick-walled cylinder) and a chamber inside in which a turbulent flow of steam entered at 95 °C, which increased its temperature through convection due to the transfer of heat through the walls of the kiln. For the solid section, the outer wall of the reactor was considered a boundary condition, and an automatic meshing was carried out using the ANSYS Student Version 2020R software, with a solid–liquid interface between the steam flow and the reactor. The dimensions of the geometry used are shown in Figure 5.

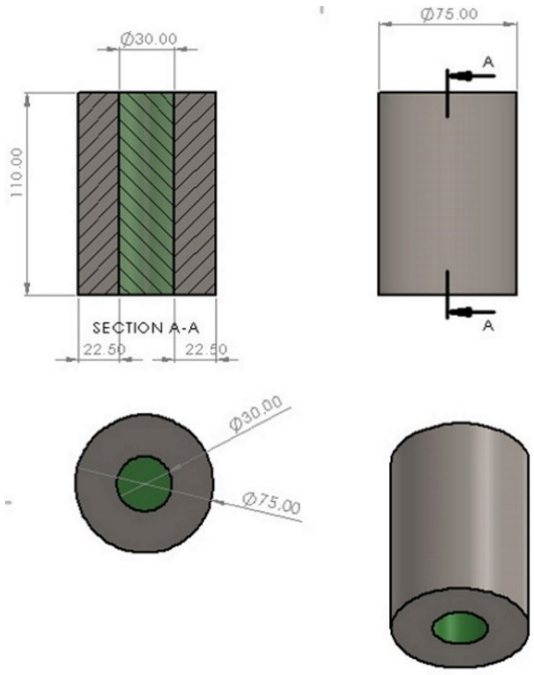

Figure 5. Geometry and dimensions of the reactor.

4. Conclusions

In this study, it was possible to design a gasification reactor to produce hydrogen, which improved the hydrogen/carbon monoxide ratio to a value of 6.67. The highest percentage of selectivity toward hydrogen production was 51.8, which was achieved at a reaction temperature of 368 °C, a reaction time of 90 min, and atmospheric pressure. It was also found that the Ni catalyst favors the production of hydrogen and the reduction in CO_2 and CO since if we compare the reaction without catalysts versus the catalyzed reaction, the increase in the percentage of hydrogen was 26%. In addition, catalysts in the range of 1.5–5% Ni supported on Al_2O_3 were studied, and it can be concluded that the best results were achieved with the 2.5% by weight Ni catalyst.

Regarding the calculation of the calorific power of the syngas obtained in the best reaction conditions, although this is lower than commercial LPG, its value was increased

owing to the use of catalysts. To expand on this study, it is recommended to compare the values obtained through this calculation through experiments.

In the simulation process, the values obtained were similar to the real values, presenting an error of 0.06% in the steady-state model. Regarding the model of the reactor in a transitory state, it was found that the value of the temperature on the internal surface of the reactor was equal to 509 °C. In addition, the temperature values of the gasses produced tend to coincide with the values obtained through simulation and experimentation over time. Therefore, the numerical methodologies developed in steady and transitory states are useful to obtain new information by changing the conditions without requiring experimental processes.

Author Contributions: Conceptualization, S.Z. and A.M.-I.; methodology, D.T.; software, P.Á.; validation, L.J.; investigation D.T.; writing—original draft preparation, C.A. and M.A.-G.; writing—review and editing, V.P.-V. and L.J.; supervision, S.Z. and A.M.-I. All authors have read and agreed to the published version of the manuscript.

Funding: This research was funded by DIUC—Universidad de Cuenca in the Project "Producción de hidrógeno a partir de la biomasa procedente de los residuos de la planta de banano mediante gasificación catalítica en agua en condiciones subcrítica".

Institutional Review Board Statement: Not applicable.

Informed Consent Statement: Not applicable.

Conflicts of Interest: The authors declare no conflict of interest.

References

1. Shayan, E.; Zare, V.; Mirzaee, I. Hydrogen production from biomass gasification; a theoretical comparison of using different gasification agents. *Energy Convers. Manag.* **2018**, *159*, 30–41. [CrossRef]
2. Bhavanam, A.; Sastry, R.C. Biomass Gasification Processes in Downd raft Fixed Bed Reactors: A Review. *Int. J. Chem. Eng. Appl.* **2011**, *2*, 425–433. [CrossRef]
3. Yakaboylu, O.; Harinck, J.; Smit, K.G.; De Jong, W. Supercritical Water Gasification of Biomass: A Literature and Technology Overview. *Energies* **2015**, *8*, 859–894. [CrossRef]
4. International Energy Agency. *Global Hydrogen Review 2021*; OECD Publishing París: Paris, France, 2021. [CrossRef]
5. Rahmouni, S.; Negrou, B.; Settou, N.; Dominguez, J.; Gouareh, A. Prospects of hydrogen production potential from renewable resources in Algeria. *Int. J. Hydrogen Energy* **2017**, *42*, 1383–1395. [CrossRef]
6. Ishaq, H.; Dincer, I. Comparative assessment of renewable energy-based hydrogen production methods. *Renew. Sustain. Energy Rev.* **2021**, *135*, 110192. [CrossRef]
7. Zhang, Y.; Li, L.; Xu, P.; Liu, B.; Shuai, Y.; Li, B. Hydrogen production through biomass gasification in supercritical water: A review from exergy aspect. *Int. J. Hydrogen Energy* **2019**, *44*, 15727–15736. [CrossRef]
8. Noussan, M.; Raimondi, P.P.; Scita, R.; Hafner, M. The Role of Green and Blue Hydrogen in the Energy Transition—A Technological and Geopolitical Perspective. *Sustainability* **2020**, *13*, 298. [CrossRef]
9. Atilhan, S.; Park, S.; El-Halwagi, M.M.; Atilhan, M.; Moore, M.; Nielsen, R.B. Green hydrogen as an alternative fuel for the shipping industry. *Curr. Opin. Chem. Eng.* **2021**, *31*, 100668. [CrossRef]
10. Howarth, R.W.; Jacobson, M.Z. How green is blue hydrogen? *Energy Sci. Eng.* **2021**, *9*, 1676–1687. [CrossRef]
11. Kim, S.-H.; Kumar, G.; Chen, W.-H.; Khanal, S.K. Renewable hydrogen production from biomass and wastes (ReBioH2-2020). *Bioresour. Technol.* **2021**, *331*, 125024. [CrossRef]
12. Anniwaer, A.; Chaihad, N.; Zhang, M.; Wang, C.; Yu, T.; Kasai, Y.; Abudula, A.; Guan, G. Hydrogen-rich gas production from steam co-gasification of banana peel with agricultural residues and woody biomass. *Waste Manag.* **2021**, *125*, 204–214. [CrossRef] [PubMed]
13. Singh, V.; Das, D. Potential of Hydrogen Production from Biomass. In *Science and Engineering of Hydrogen-Based Energy Technologies*; Elsevier: West Bengal, India, 2019; pp. 123–164. [CrossRef]
14. Baharuddin, N.A.; Yusoff, W.N.A.W.; Aziz, A.J.A.; Tahir, N.N.M. Hydrogen fuel cells for sustainable energy: Development and progress in selected developed countries. *IOP Conf. Ser. Mater. Sci. Eng.* **2021**, *1078*, 012011. [CrossRef]
15. Nuttall, W.J.; Bakenne, A.T. The Future of Energy and Mobility. In *Fossil Fuel Hydrogen*; Springer International Publishing: Cham, Switzerland, 2020; pp. 15–31. [CrossRef]
16. Wu, C.; Dong, L.; Onwudili, J.; Williams, P.T.; Huang, J. Effect of Ni Particle Location within the Mesoporous MCM-41 Support for Hydrogen Production from the Catalytic Gasification of Biomass. *ACS Sustain. Chem. Eng.* **2013**, *1*, 1083–1091. [CrossRef]
17. Pang, Y.; Yu, D.; Chen, Y.; Jin, G.; Shen, S. Hydrogen production from steam gasification of corn straw catalyzed by blast furnace gas ash. *Int. J. Hydrogen Energy* **2020**, *45*, 17191–17199. [CrossRef]

18. Yao, D.; Hu, Q.; Wang, D.; Yang, H.; Wu, C.; Wang, X.; Chen, H. Hydrogen production from biomass gasification using biochar as a catalyst/support. *Bioresour. Technol.* **2016**, *216*, 159–164. [CrossRef] [PubMed]
19. Gao, N.; Li, A.; Quan, C.; Gao, F. Hydrogen-rich gas production from biomass steam gasification in an updraft fixed-bed gasifier combined with a porous ceramic reformer. *Int. J. Hydrogen Energy* **2008**, *33*, 5430–5438. [CrossRef]
20. Li, J.; Yin, Y.; Zhang, X.; Liu, J.; Yan, R. Hydrogen-rich gas production by steam gasification of palm oil wastes over supported tri-metallic catalyst. *Int. J. Hydrogen Energy* **2009**, *34*, 9108–9115. [CrossRef]
21. Cerone, N.; Zimbardi, F.; Contuzzi, L.; Baleta, J.; Cerinski, D.; Skvorčinskienė, R. Experimental investigation of syngas composition variation along updraft fixed bed gasifier. *Energy Convers. Manag.* **2020**, *221*, 113116. [CrossRef]
22. Jin, K.; Ji, D.; Xie, Q.; Nie, Y.; Yu, F.; Ji, J. Hydrogen production from steam gasification of tableted biomass in molten eutectic carbonates. *Int. J. Hydrogen Energy* **2019**, *44*, 22919–22925. [CrossRef]
23. Tomczak, W.; Ferrasse, J.-H.; Giudici-Orticoni, M.-T.; Soric, A. Effect of hydraulic retention time on a continuous biohydrogen production in a packed bed biofilm reactor with recirculation flow of the liquid phase. *Int. J. Hydrogen Energy* **2018**, *43*, 18883–18895. [CrossRef]
24. Arena, U. Process and technological aspects of municipal solid waste gasification. A review. *Waste Manag.* **2012**, *32*, 625–639. [CrossRef] [PubMed]
25. Ruiz, J.; Juárez, M.; Morales, M.; Muñoz, P.; Mendívil, M. Biomass gasification for electricity generation: Review of current technology barriers. *Renew. Sustain. Energy Rev.* **2013**, *18*, 174–183. [CrossRef]
26. Puig-Arnavat, M.; Bruno, J.C.; Coronas, A. Review and analysis of biomass gasification models. *Renew. Sustain. Energy Rev.* **2010**, *14*, 2841–2851. [CrossRef]
27. Basu, P. *Biomass Gasification and Pyrolysis: Practical Design and Theory*; Academic Press: Burlington, MA, USA, 2010.
28. Zhang, L.; Xu, C.C.; Champagne, P. Overview of recent advances in thermo-chemical conversion of biomass. *Energy Convers. Manag.* **2010**, *51*, 969–982. [CrossRef]
29. Anukam, A.; Mamphweli, S.; Reddy, P.; Meyer, E.; Okoh, O. Pre-processing of sugarcane bagasse for gasification in a downdraft biomass gasifier system: A comprehensive review. *Renew. Sustain. Energy Rev.* **2016**, *66*, 775–801. [CrossRef]
30. Dascomb, J.; Krothapalli, A.; Fakhrai, R. Thermal conversion efficiency of producing hydrogen enriched syngas from biomass steam gasification. *Int. J. Hydrogen Energy* **2013**, *38*, 11790–11798. [CrossRef]
31. Salam, M.A.; Ahmed, K.; Akter, N.; Hossain, T.; Abdullah, B. A review of hydrogen production via biomass gasification and its prospect in Bangladesh. *Int. J. Hydrogen Energy* **2018**, *43*, 14944–14973. [CrossRef]
32. Zhang, G.; Liu, H.; Wang, J.; Wu, B. Catalytic gasification characteristics of rice husk with calcined dolomite. *Energy* **2018**, *165*, 1173–1177. [CrossRef]
33. Sun, J.; Xu, L.; Dong, G.-H.; Nanda, S.; Li, H.; Fang, Z.; Kozinski, J.A.; Dalai, A.K. Subcritical water gasification of lignocellulosic wastes for hydrogen production with Co modified Ni/Al2O3 catalysts. *J. Supercrit. Fluids* **2020**, *162*, 104863. [CrossRef]
34. Lu, Y.; Jin, H.; Zhang, R. Evaluation of stability and catalytic activity of Ni catalysts for hydrogen production by biomass gasification in supercritical water. *Carbon Resour. Convers.* **2019**, *2*, 95–101. [CrossRef]
35. Artetxe, M.; Alvarez, J.; Nahil, M.A.; Olazar, M.; Williams, P. Steam reforming of different biomass tar model compounds over Ni/Al_2O_3 catalysts. *Energy Convers. Manag.* **2017**, *136*, 119–126. [CrossRef]
36. Kurkela, E.; Kurkela, M.; Hiltunen, I. Production of Synthesis Gas from Biomass Residues by Staged Fixed-bed Gasification—Results from Pilot Test Campaigns. *Chem. Eng. Trans.* **2021**, *86*, 7–12. [CrossRef]
37. Narvaez, N.; Freddy, E. *Simulacion Numérica de Flujo de Aire y Transferencia de Calor en un Enfriador Vertical con Puerta Panorámica*; Publicaciones UPS: Cuenca, Ecuador, 2018.
38. Di Nardo, A.; Calchetti, G.; Bassano, C.; Deiana, P. CO_2 methanation in a shell and tube reactor CFD simulations: High temperatures mitigation analysis. *Chem. Eng. Sci.* **2021**, *246*, 116871. [CrossRef]
39. Hwang, J.G.; Choi, M.K.; Choi, D.H.; Choi, H.S. Quality improvement and tar reduction of syngas produced by bio-oil gasification. *Energy* **2021**, *236*, 121473. [CrossRef]
40. Putra, A.E.E.; Amaliyah, N.; Nomura, S.; Rahim, I. Plasma generation for hydrogen production from banana waste. *Biomass-Convers. Biorefinery* **2020**, *12*, 441–446. [CrossRef]
41. Nathoa, C.; Sirisukpoca, U.; Pisutpaisal, N. Production of Hydrogen and Methane from Banana Peel by Two Phase Anaerobic Fermentation. *Energy Procedia* **2014**, *50*, 702–710. [CrossRef]
42. de Lasa, H.; Salaices, E.; Mazumder, J.; Lucky, R. Catalytic Steam Gasification of Biomass: Catalysts, Thermodynamics and Kinetics. *Chem. Rev.* **2011**, *111*, 5404–5433. [CrossRef]
43. Gupta, E.S.K. *Engineering Thermodynamics*, 2nd ed.; S. Chand Pulishing: Nueva Delhi, India, 2019.
44. REPSOL. *Ficha de Seguridad GLP*; Refinería La Pampilla S.A.A: Callao, Peru, October 2016.
45. Lojagas. Hoja de seguridad del Gas Licuado de Petroleo. Loja, NÚMERO CAS*: 68476-85-7. Available online: http://lojagas.com/nueva/wp-content/uploads/2017/08/G-99.-HOJA-DE-SEGURIDAD-GAS-LICUADO-DE-PETROLEO.pdf (accessed on 26 February 2022).
46. Rievaj, V.; Gaňa, J.; Synák, F. Is hydrogen the fuel of the future? *Transp. Res. Procedia* **2019**, *40*, 469–474. [CrossRef]
47. Parthasarathy, P.; Narayanan, K.S. Hydrogen production from steam gasification of biomass: Influence of process parameters on hydrogen yield—A review. *Renew. Energy* **2014**, *66*, 570–579. [CrossRef]

48. International Energy Agency. Net Zero by 2050. A Roadmap for the Global Energy Sector. October 2021. Available online: www.iea.org (accessed on 14 March 2022).
49. Ferrerira da Silva, I.; Reis Fontinelle Souto, I.; Collins, S.R.A.; Elliston, A.; de Queriroz, J.H.; Waldron, K.W. Impact of Hot Water and Alkaline Pre-treatments in Cellulosic Ethanol Production from Banana Pseudostem. *Bioenerg Res.* **2020**, *13*, 1159–1170. [CrossRef]
50. Eyvaz, M.; Yüksel, E. (Eds.) *Desalination and Water Treatment*; InTech: Houston, TX, USA, 2018. [CrossRef]
51. Onsan, Z.I.; Avci, A.K. *Multiphase Catalytic Reactors: Theory, Design, Manufaturing, and Applications*; John Wiley & Sons: Hoboken, NJ, USA, 2016.
52. Lima, D.S.; Calgaro, C.O.; Perez-Lopez, O.W. Hydrogen production by glycerol steam reforming over Ni based catlysts prepared by different methods. *Biomas Bioenergy* **2019**, *130*, 105358. [CrossRef]
53. Ghassemi, M.; Kamvar, M.; Steinberger, W.R. *Fundamentals of Heat and Fluid Flow in High Temperature Fuel Cells*, 1st ed.; Academic Press: Cambridge, MA, USA, 2020.